Spin-orbit coupling and surface magnetism coexisting in spin-dependent low-energy He^+-ion surface scattering

T. T. Suzuki[1,*] and O. Sakai[1,2]

[1]*National Institute for Materials Science, 1-1 Namiki, Tsukuba, Ibaraki 305-0047, Japan*

[2]*Comprehensive Research Organization for Science and Society, Kamitakazu 1601, Tsuchiura, Ibaraki 300-0811, Japan*

(Received 26 January 2017; revised manuscript received 30 March 2017; published 24 April 2017)

Surface magnetism is analyzed by spin-dependent He^+-ion neutralization (the Auger neutralization) in the vicinity of a surface using an electron spin-polarized low-energy He^+-ion beam [spin-polarized ion scattering spectroscopy (SP-ISS)]. Recently, spin-orbit coupling (SOC) has been found to act as another mechanism of spin-dependent low-energy He^+-ion scattering. Thus, it is crucial for surface magnetism analyses by SP-ISS to separate those two mechanisms. In the present study, we investigated the spin-induced asymmetry in scattering of low-energy He^+ ions on ultrathin Au and Sn films as well as the oxygen adsorbate on a magnetized-Fe(100) surface where these two mechanisms may coexist. We found that the Fe surface magnetism immediately disappeared with the growth of those overlayers. On the other hand, we observed no induced spin polarization in the Au and Sn thin films even in the very initial stage of the growth. We also observed that the spin asymmetry of the O adsorbate was induced by the magnetism of the underlying Fe substrate. The present study demonstrates that the two mechanisms of the spin-asymmetric He^+-ion scattering (the ion neutralization and SOC) can be separated by an azimuthal-angle-resolved SP-ISS measurement.

DOI: 10.1103/PhysRevB.95.155437

I. INTRODUCTION

He^+-ion beams have been widely used as a probe for solid-surface analysis. This is because the ionization energy of He is so large at 24.6 eV, which is actually the largest among all elements, and, consequently, He^+ ions are neutralized with high probability in the vicinity of the surfaces. This is especially the case for low collisional energy (i.e., below a few keV) between the He^+ ion and a surface. The velocity of He^+ ions is comparable to the Fermi velocity at such low energy, hence the low-energy He^+ ion has sufficient duration for the charge exchange with a surface. Therefore, the outermost surface can be selectively analyzed by detecting the scattered low-energy He^+ ion which survives the neutralization low-energy He^+-ion scattering spectroscopy [low-energy ion scattering spectroscopy (LEIS) or ion scattering spectroscopy (ISS)] [1,2].

It is well known that the low-energy He^+ ion is typically neutralized in the vicinity of surfaces through the Auger neutralization (AN) mechanism, which is an interatomic Auger process [Fig. 1(a)] [1]. Due to the Pauli exclusion principle, the electron-spin orientation of the He^+ ion, which is defined by the 1*s* electron, should be opposite to that of the surface electron involved in the AN [3]. Thus, the AN probability reflects the population density of the surface valence electrons which have an opposite direction spin to the impinging He^+ ion. In other words, the spin-dependent He^+-ion scattering is related to surface spin polarization, namely, the surface magnetism. This is a basic principle of surface spin polarization analysis by spin-polarized ISS (SP-ISS) [4].

In SP-ISS, the scattered He^+-ion intensity is measured separately for the incident He^+ ion with up and down spins by using a spin-polarized He^+-ion beam. The spin dependence of the He^+-ion scattering is evaluated by the spin asymmetry A defined as $(I_\uparrow - I_\downarrow)/[P_{He+} \cdot (I_\uparrow + I_\downarrow)]$, where $I_\uparrow$ and $I_\downarrow$ are the scattered intensities of the incident He^+ ions with up and down spin, respectively, and P_{He+} denotes the spin polarization of the incident He^+ ion beam. The direction of the up spin (the down spin) is defined to be parallel (antiparallel) to the guiding magnetic field (Fig. 2). We have applied SP-ISS to the spin-polarization analysis of various magnetic surfaces in the past decade [5].

Aside from the above-mentioned ion neutralization-based mechanism, we have indicated that spin-dependent He^+-ion scattering also arises due to the spin-orbit coupling (SOC) in the He^+-target atom collision [6–9]. This claim is based on the observation of spin-dependent He^+-ion scattering on nonmagnetic surfaces which consists of relatively heavy elements. The large spin asymmetry of more than 10% has been observed in those experiments, which was not attributed to the spin-dependent He^+-ion neutralization because of no spin polarization on nonmagnetic surfaces. The alternative mechanism, which is the SOC of the He^+-ion scattering, is intuitively interpreted as the effect on the spin $\mathbf{S}$ of the projectile He^+ ion from the Biot-Savart field $\mathbf{H}$ induced by the projectile He^+ ion angular motion around the target nucleus during the He^+-target atom binary collision. Thus, the SOC potential U_{SOC} in the collision between a projectile of mass M_1 and a target of atomic number Z_2 has the following form:

$$U_{\mathrm{SOC}} = \mathbf{H} \cdot \mathbf{S} \propto (Z_2/|\mathbf{r}|^3)(\mathbf{r} \times M_1\mathbf{v}) \cdot \mathbf{S}, \qquad (1)$$

where $\mathbf{v}$ is the velocity of the projectile and $\mathbf{r}$ is the position of the target nucleus as seen from the projectile. It is noted that the He^+-ion spin is presumed to accompany the nucleus motion of the He^+ ion during the collision in the simple picture expressed in Eq. (1).

Recently, we have theoretically shown that SOC for the hole virtually created in the target atom during the collision is responsible for the spin-dependent He^+-ion scattering on

*Corresponding author: suzuki.taku@nims.go.jp

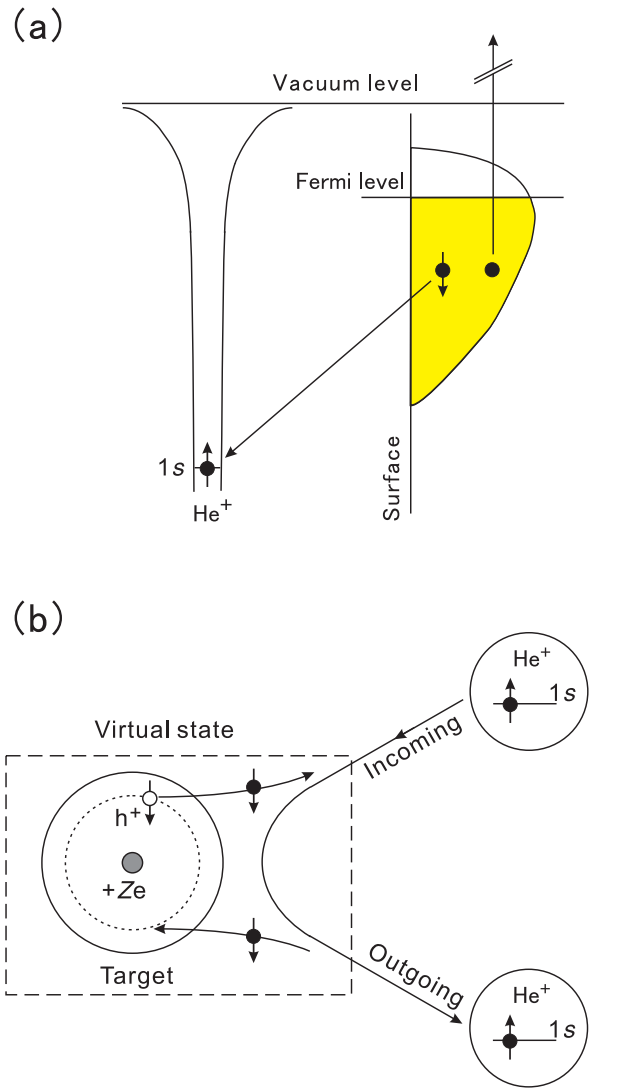

FIG. 1. Two mechanisms of the spin-dependent low-energy He^+-ion scattering on solid surfaces. (a) In the Auger neutralization, the hole of the He^+ 1s orbital is filled by a surface electron with opposite spin to that of the He^+ 1s electron. (b) Due to spin-orbit coupling for a hole virtually created in a target atom during the collisional intermediate state, the scattering cross section of a He^+ ion differs between spins.

nonmagnetic surfaces [Fig. 1(b)] [10]. The SOC in the collisional intermediate state explains the large spin asymmetry of more than 10%, which could not be understood if the He^+-ion spin was presumed to classical mechanically accompany the He^+-ion nuclear motion during the collision as the simple picture given by Eq. (1).

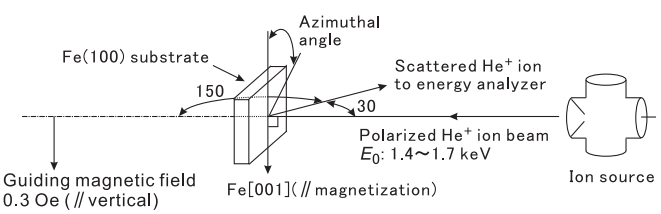

FIG. 2. Schematic of the experimental setup.

The two mechanisms of the spin-dependent He^+-ion scattering, i.e., spin-dependent ion neutralization and SOC, have been separately investigated so far. No study has been reported for the situation where surface magnetism and SOC coexist. Thus, it remains an open question as to how those two mechanisms can be separated experimentally, although it is quite important for surface spin-polarization analysis by SP-ISS.

In the present study, we investigated spin-dependent He^+-ion scattering on the surface where the effects of surface magnetism and SOC were expected to coexist. As a sample, we selected an ultrathin Sn or Au film on a magnetized Fe single-crystalline substrate. Our earlier studies have revealed that the He^+-ion scattering is significantly spin dependent due to SOC on a polycrystalline Sn or Au sheet target [8,9]. On the other hand, the effect of surface magnetism in the He^+-ion scattering may appear on an ultrathin nonmagnetic film grown on a magnetized substrate due to the induced spin polarization. It has been suggested that magnetic spin polarization is induced in the conduction electrons of the nonmagnetic overlayer at the interface with a magnetic substrate [11–17]. For the sake of comparison, we also investigated the O/Fe system in the present study, where the spin-dependent scattering from O is considered to be mostly due to the surface spin polarization. This is because we have observed no spin asymmetry at the O peak position on the Fe(100) surface heavily exposed to the O_2 atmosphere in our previous SP-ISS study [4]. The negligibly small contribution of SOC in the He^+-ion O-atom collision will be evidenced from the azimuthal-angle dependence of the spin-asymmetric He^+-ion scattering from O in the last part of our paper.

II. EXPERIMENT

We performed experiments in an ultrahigh vacuum (UHV) chamber (base pressure $\sim 7 \times 10^{-9}$ Pa), which was equipped with a rotatable electrostatic energy analyzer, a beam line for spin-polarized $^4He^+$ ions, a sample manipulator, a reflection high-energy electron diffraction (RHEED) apparatus, deposition sources of Fe, Au, and Sn, and a quartz oscillator thickness monitor. Electron-spin-polarized $^4He^+$ ions were generated by the Penning ionization of spin-polarized metastable He 2^3S_1 atoms [4]. We used an optical pumping technique to polarize metastable He 2^3S_1 atoms. The polarization of the incident He^+-ion beam (P_{He^+}) is defined as $(n_\uparrow - n_\downarrow)/(n_\uparrow + n_\downarrow)$, where $n_\uparrow$ and $n_\downarrow$ are the numbers of projectile He^+ ions whose magnetic moment is parallel and antiparallel to the guiding magnetic field, respectively. The spin polarization of the He^+-ion beam P_{He+} in the present experiment was about 0.2 [18].

The entire apparatus was surrounded by a three-axis coil to compensate the Earth's magnetic field. An additional coil produced a weak guiding field (0.3 Oe), which was parallel to the vertical axis (Fig. 2). The spin direction of the incident He^+-ion beam was defined by the guiding magnetic field; hence, it was polarized so as to be parallel or antiparallel to the guiding field. We set the scattering geometry as the spin of the incident He^+ ion to be perpendicular to both the scattering plane and the surface normal of the Fe(100) target, as shown in Fig. 2. In the present SP-ISS experiment, the incident and exit

angles measured from the surface normal direction of the target were 0° and 30°. Thus, the scattering angle was 150°. The incident energy E_0 was in the range between 1.4 and 1.7 keV.

The scattered He^+ ions were measured using a rotatable hemispherical energy analyzer (Omicron SHA50), which was operated in a constant pass-energy mode with a pass energy of 318 eV. The SP-ISS spectra for the two opposite spins of the incident He^+ ion (i.e., up and down spins) were alternately measured more than 100 times in order to eliminate the effect of changes with time. The signals were separately accumulated for the up and down spin-polarized He^+ ions and, finally, they were compared to each other to obtain the spin asymmetry A.

Iron single-crystalline (100) films (bcc-Fe) were epitaxially grown on MgO(100) substrates by vapor deposition of iron [19]. The thickness of the Fe film was a few tens of nanometers. We deposited Sn and Au on the Fe(100) film using an electron-beam evaporator (Omicron EFM3) at room temperature in UHV. The typical deposition rate was 0.05 nm/min. The sample was pulse magnetized in-plane by a retractable pulse magnet placed in the UHV chamber before the SP-ISS measurements. The magnetization direction was parallel to the Fe[001] easy axis of the bcc-Fe films, which was parallel to the vertical direction as shown in Fig. 2.

III. RESULTS AND DISCUSSION

Figure 3(a) shows the spin asymmetries of Fe and Au as a function of the Au deposition amount on the Fe(100) surface. The spin asymmetries of Fe and Au were measured at the ISS peak energies, which were 1135 and 1400 eV, respectively. Since the ISS peaks of Fe and Au are well separated, as shown in the inset of Fig. 3(a), the spin asymmetries of Fe and Au are straightforwardly attributed to the collision of the He^+ ion to the Fe and Au target atoms at the Au/Fe surface, respectively.

In our RHEED experiment, we consistently observed a 1×1 streak through the Au deposition on the Fe(100) surface, although the streaks became slightly obscured with the Au deposition. This suggests the growth of the Au overlayer

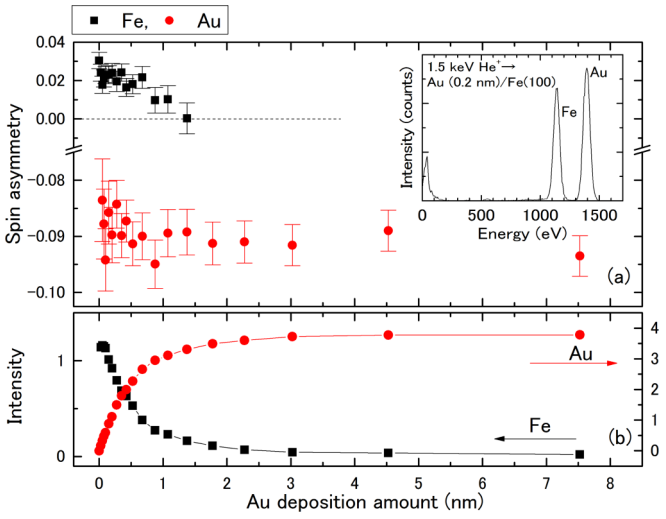

FIG. 3. (a) The spin asymmetry and (b) the scattered He^+-ion intensity of Fe (black squares) and Au (red circles) as a function of the Au deposition amount on the magnetized-Fe(100) substrate. The inset shows the ISS spectrum of the Au (0.2 nm)/Fe(100) surface.

with a similar crystalline periodicity to Fe(100). In fact, it has been reported that Au(100) epitaxially grows on Fe(100) with a rotation of 45° due to good lattice matching, namely, Au(100)//Fe(100) and Au[110]//Fe[100] [20–22]. Thus, we hereafter assume that one monolayer (ML) of the Au overlayer has a thickness of half of the lattice constant (0.204 nm).

Figure 3(b) shows the behavior of the ISS signal intensity at the peak position of Fe and Au as a function of the Au deposition amount. The ISS signal intensity is integrated in counts from 1120 to 1160 eV for Fe and from 1375 to 1415 eV for Au. The Fe signal vanishes with the Au deposition of about 3.5 nm. By considering the surface sensitivity of ISS, the Fe surface should be fully covered by the Au deposition of 3.5 nm. Thus, it seems that the layer-by-layer growth does not explain our data in Fig. 3(b). However, it has been indicated that the Au film grows on Fe(100) with nearly layer by layer at the substrate temperature of 373 K [20]. The inconsistency on the growth mode of Au/Fe(100) may be due to the Fe substrate temperature during the Au film growth. It was room temperature in our case and, consequently, the thermally activated diffusion process at the surface is limited as statistical growth [23]. The effect of reduced interlayer mass transport during the film growth analyzed by ISS has been discussed by Primetzhofer *et al.* [24]. In the statistical growth, the full covered surface is reached exponentially as a function of the mean thickness of the deposited film, and it is interpreted to be the case of Au/Fe(100) in the present study.

In Fig. 3(a), the spin asymmetry of Fe decreases with the Au deposition, and it finally disappears at the thickness of several ML. This behavior of the Fe spin asymmetry is interpreted to be due to the bonding at the Au/Fe interface from the analogy of O/Fe discussed later. Thus, the hybridization of the electronic state at the Au/Fe interface depolarizes the spin state of the Fe surface. No magnetic order is observed in the Au thin film in the whole thickness range as discussed below; therefore, no antiferromagnetic coupling of Au at the Au/Fe interface is observed, which has been proposed to be the origin of the magnetic dead layer at the magnetic/nonmagnetic interface [25–28].

On the other hand, the spin asymmetry of Au continuously exhibits the opposite polarity to the spin asymmetry of Fe. No substantial change of the Au spin asymmetry occurs in the whole thickness range. The spin asymmetry of Au on the Au thick film should be due to SOC because of no effect of magnetism from the Fe substrate. Actually, the spin asymmetry of Au on the thick film is equivalent to that on the polycrystalline Au sheet observed in our earlier study [6].

The behavior of the spin asymmetry observed on Au/Fe in Fig. 3(a) is similar to that on Sn/Fe, as shown in Fig. 4(a). In the case of Sn/Fe, it is additionally observed that the spin asymmetry of Sn is slightly enhanced in the initial stage of the Sn deposition. No substantial change occurs in the spin asymmetry of Sn by the further deposition of Sn. Similarly to Au/Fe, the spin asymmetry of Sn on the thick Sn film is equivalent to that observed on the polycrystalline Sn sheet [9]; hence, it is attributed to the pure SOC effect. Those similar behaviors of the spin asymmetry between Au/Fe and Sn/Fe suggest that the origin of the spin asymmetry is identical in these two systems.

In our RHEED experiment on Sn/Fe, we observed transmission patterns indicating the Sn island formation on the Fe

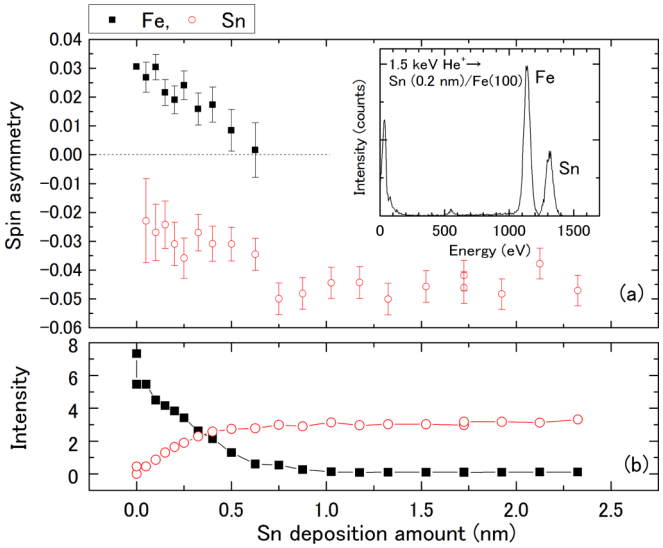

FIG. 4. (a) The spin asymmetry and (b) the scattered He^+-ion intensity of Fe (solid black squares) and Sn (open red circles) as a function of the Sn deposition amount on the magnetized-Fe(100) substrate. The inset shows the ISS spectrum of the Sn (0.2 nm)/Fe(100) surface.

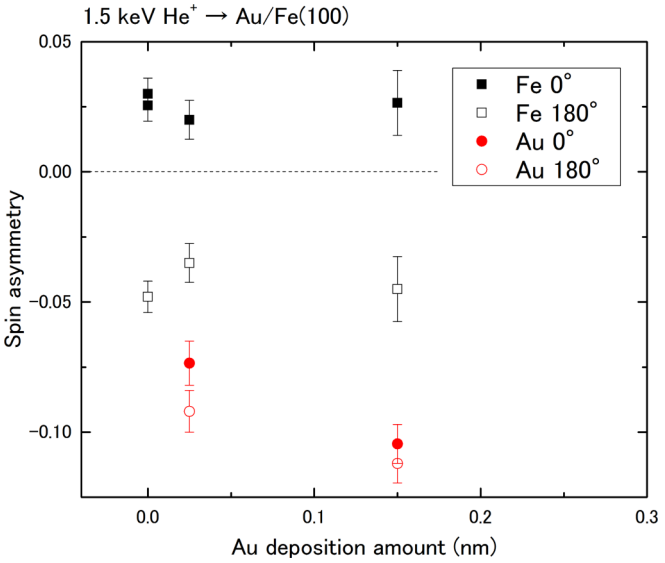

FIG. 5. The spin asymmetry of Fe (black squares) and Au (red circles) in the very initial stage of the Au deposition on the magnetized-Fe(100) substrate. The asymmetries are plotted for the azimuthal angles of 0° and 180°.

surface in the initial stage of the growth. The behavior of the ISS signal intensity as a function of the Sn deposition amount is shown in Fig. 4(b). The ISS signal intensity is integrated in counts from 1120 to 1160 eV for Fe and from 1285 to 1325 eV for Sn. The behavior of the ISS signal intensity as a function of the deposition amount of Sn/Fe(100) is similar to that of Au/Fe(100) [Fig. 3(b)], and thus it is likely that the growth mode is similar between Au/Fe(100) and Sn/Fe(100), which is the statistical growth.

It is well known that the quasiresonance charge transfer is a major channel of the He^+-ion neutralization in addition to AN on Sn surfaces [1]. The quasiresonance neutralization (qRN) takes place because a Sn atom has a $4d$ core level which is energetically close to the empty $1s$ level of a He^+ ion. As evidence of qRN on Sn, both the scattered He^+-ion intensity and the spin asymmetry of Sn periodically oscillates as a function of the reciprocal of the He^+-ion velocity [9,29–31]. Those oscillations are understood in terms of the quantum mechanical interference between adiabatic and nonadiabatic transitions in the quasiresonance charge transfer.

It is noted that the valence electron that is responsible for the spin polarization, i.e., magnetism, is not involved in the qRN of the He^+ ion because the He^+ $1s$ level is energetically as deep as 24.6 eV, as measured from the vacuum level. Thus, the spin polarization in the Sn ultrathin film induced by the underlying Fe substrate is not detected through qRN. This is not the case for the He^+-Au collision, where only AN is a major neutralization channel of the He^+ ion. It is known that the collision-induced neutralization/reionization is negligible compared to AN in the He^+-Au system [32], although it has been indicated to be significant at the much higher energies used in the present study [33]. Therefore, the effect of the target spin polarization should appear more strikingly in the spin asymmetry on Au rather than on Sn. Nevertheless, the increase of the spin asymmetry in the initial stage of the thin-film growth is much pronounced on Sn than on Au. This implies that the variation of the spin asymmetry of Sn in the initial stage of the deposition is simply due to SOC. In other words, no induced spin polarization appears in the nonmagnetic overlayer by the magnetism of the underlying substrate in both the systems of Sn/Fe(100) and Au/Fe(100).

To examine the above interpretation, the relationship between the spin asymmetry and the azimuthal angle was investigated in the very initial stage of the Au deposition on Fe(100), as shown in Fig. 5. The spin asymmetry originating from SOC is independent of azimuthal angle because it arises from the He^+-ion target atom binary collision [7]. On the other hand, the asymmetry by the magnetism is proportional to the cosine of the angle between the He^+-ion spin and the target magnetization [34]. Since the He^+-ion spin is parallel or antiparallel to the guiding field, the spin asymmetry A originating from the magnetism is related to the azimuth rotation angle δ as $A \propto \cos\delta$. Therefore, if the effect of SOC is additionally considered, the spin asymmetry A is expressed as

$$A \propto \cos\delta + c, \tag{2}$$

where c is the offset due to SOC.

The polarity of the spin asymmetry should reverse by the azimuthal-angle rotation of 180° if the contribution of SOC is relatively small, as shown in Eq. (2). Actually, the polarity of the Fe asymmetry is opposite to each other between the azimuth angle of 0° and 180° in Fig. 5. By contrast, no substantial change occurs in the spin asymmetry of Au by rotating the azimuth angle. This manifests that the spin asymmetry of Au purely originates from SOC in the whole thickness range, including the very initial stage of the Au deposition.

It is observed in Fig. 5 that the absolute value of the Fe asymmetry differs slightly between the azimuth angles of 0° and

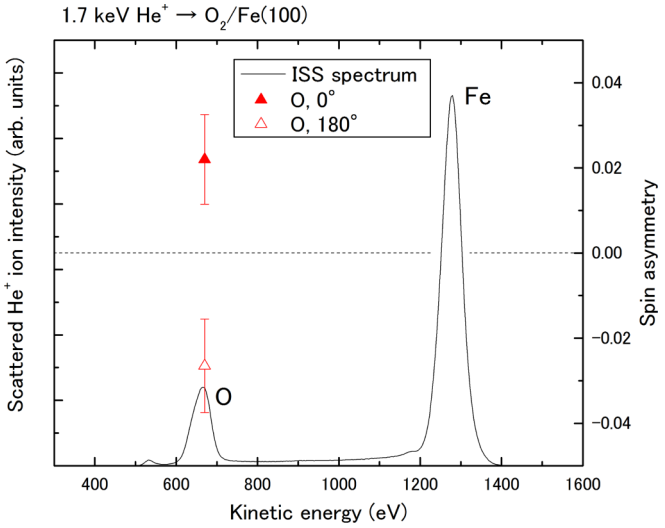

FIG. 6. The ISS spectrum (solid black curve) and the spin asymmetry of oxygen measured at the azimuthal angles of 0° (solid red triangle) and 180° (open red triangle). The sample was the magnetized-Fe(100) substrate exposed to an O_2 atmosphere of 1.33×10^{-5} Pa for 50 s at room temperature.

180°. According to Eq. (2), if the spin asymmetry entirely originates from the magnetism, the absolute values should agree with each other between those azimuth angles. Therefore, the azimuthal-angle dependence of the Fe asymmetry shows the slight contribution of SOC to the spin asymmetry of Fe.

As a general trend, we have observed that the effect of SOC increases with the mass of the He^+ ion's collision-partner atom [8]. The slight effect of SOC found on Fe in the present study is consistent with this tendency. The relationship between the target atomic number and SOC is not understood by the classical mechanical picture expressed in Eq. (1). This is because the charge of the target nucleus increases as the target atomic mass increases, but, simultaneously, the distance between the He^+ ion and the target nucleus increases with the enhanced screened Coulomb force. Therefore, SOC in the collision-induced quantum mechanical intermediate state described in Sec. I should be considered to understand the target element dependence of SOC. This will be our future work.

In agreement with the trend of the target element dependence of SOC mentioned above, we observed no effect of SOC in the He^+-ion oxygen-adatom collision, as shown in Fig. 6. The O/Fe(100) surface was prepared by exposing the Fe(100) surface to an oxygen (O_2) atmosphere with a partial pressure of 1.33×10^{-5} Pa for 50 s at room temperature. It has been indicated that atomic oxygen adsorbs on Fe(100) as a result of the dissociation of the O_2 molecule [35]. The behavior of the spin asymmetry of Fe and O as a function of the exposure to the O_2 atmosphere has already been reported in our previous paper [34]. Briefly, both spin asymmetries of Fe and O exhibit positive polarity and they monotonically decrease with the exposure. They finally disappear when exposed at 1.33×10^{-5} Pa for 80 s. Thus, the exposure condition used in the present study corresponds to the transient surface where both of those spin asymmetries of Fe and O are changing. In Fig. 6 , the spin asymmetry of O perfectly reverses by the azimuthal-angle rotation of 180°. Thus, no offset corresponding to c in Eq. (2) is observed and, consequently, the spin asymmetry of O is simply attributed to the spin polarization induced by the magnetism of the Fe(100) substrate. The mechanism of the induced spin polarization has been proposed to be the molecular orbital hybridization between O $2p$ and Fe $3d$ [36,37].

IV. CONCLUSION

We investigated spin-dependent low-energy He^+-ion scattering in terms of the coexistence effect on the surface magnetism and the spin-orbit coupling (SOC). We examined the coexistence effect on these two mechanisms from SP-ISS experiments on the Au and Sn thin films formed on a magnetized Fe(100) substrate. We concluded that the variation of the spin asymmetry of Sn observed as a function of the thin-film thickness is attributed just to SOC. Thus, the change of the electronic state of the target atom modifies the spin asymmetry originating from SOC even though it arises from the He^+-ion target atom binary collision. The spin asymmetries of Au and Sn are attributed to SOC in the whole thickness range. In contrast, the spin asymmetry of O adsorbed on Fe(100) is attributed to just the spin polarization induced by the magnetism of the underlying Fe substrate. The present study shows that the spin asymmetry A is related to the origin of the spin-dependent He^+-ion scattering as $A = \cos\delta + c$, where δ is the azimuthal angle of the target and c is the offset determined by SOC. Thus, one is able to separate those two contributions by analyzing the relationship between A and δ. This is crucial for surface spin-polarization analyses by SP-ISS.

ACKNOWLEDGMENTS

This work was partially supported by JSPS KAKENHI Grants No. JP 15K13366, No. 15H01053, and No. 24560036.

[1] H. H. Brongersma, M. Draxler, M. de Ridder, and P. Bauer, Surf. Sci. Rep. **62**, 63 (2007).
[2] H. Niehus, W. Heiland, and E. Taglauer, Surf. Sci. Rep. **17**, 213 (1993).
[3] D. L. Bixler, J. C. Lancaster, F. J. Kontur, P. Nordlander, G. K. Walters, and F. B. Dunning, Phys. Rev. B **60**, 9082 (1999).
[4] T. Suzuki and Y. Yamauchi, Surf. Sci. **602**, 579 (2008).
[5] For example, T. T. Suzuki, H. Kuwahara, and Y. Yamauchi, Surf. Sci. **605**, 1197 (2011).
[6] T. T. Suzuki, Y. Yamauchi, and S. Hishita, Phys. Rev. Lett. **107**, 176101 (2011).
[7] S. Ichinokura, T. Hirahara, O. Sakai, S. Hasegawa, and T. T. Suzuki, Radiat. Eff. Defects Solids **169**, 1003 (2014).
[8] T. T. Suzuki, O. Sakai, S. Ichinokura, T. Hirahara, and S. Hasegawa, Nucl. Instrum. Methods Phys. Res., Sect. B **354**, 163 (2015).
[9] T. T. Suzuki and O. Sakai, Nucl. Instrum. Methods Phys. Res., Sect. B **382**, 2 (2106).

[10] O. Sakai and T. T. Suzuki, J. Phys. Soc. Jpn. (to be published).
[11] N. Hosoito, K. Kodama, and R. Yamagishi, J. Phys. Soc. Jpn. **81**, 064713 (2012).
[12] J. L. Perez-Diaz and M. C. Munoz, J. Appl. Phys. **75**, 6470 (1994).
[13] N. B. Brookes, Y. Chang, and P. D. Johnson, Phys. Rev. B **50**, 15330 (1994).
[14] M. G. Samant, J. Stohr, S. S. P. Parkin, G. A. Held, B. D. Hermsmeier, F. Herman, M. van Schilfgaarde, L.-C. Duda, D. C. Mancini, N. Wassdahl, and R. Nakajima, Phys. Rev. Lett. **72**, 1112 (1994).
[15] P. Bruno, Y. Suzuki, and C. Chappert, Phys. Rev. B **53**, 9214 (1996).
[16] Y. Suzuki, T. Katayama, W. Geerts, P. Grunberg, K. Takanashi, R. Schreiber, P. Buruno, and S. Yuasa, Mater. Res. Soc. Symp. Proc. **475**, 227 (1997).
[17] J. Unguris, R. J. Celotta, and D. T. Pierce, J. Appl. Phys. **75**, 6437 (1994).
[18] T. Suzuki and Y. Yamauchi, Phys. Rev. A **77**, 022902 (2008).
[19] Y. Yamauchi and M. Kurahashi, Appl. Surf. Sci. **169**, 236 (2001).
[20] J. Unguris, R. J. Celotta, D. A. Tulchinsky, and D. T. Pierce, J. Magn. Magn. Mater. **198**, 396 (1999).
[21] A. Brambilla, A. Calloni, G. Berti, G. Bussetti, L. Duo, and F. Ciccacci, Cryst. Res. Technol. **49**, 587 (2014).
[22] S. Voss, M. Fonin, F. Zinser, M. Burgert, U. Groth, and U. Rudiger, Polyhedron **28**, 1606 (2009).
[23] H. Brune, G. S. Bales, J. Jacobsen, C. Boragno, and K. Kern, Phys. Rev. B **60**, 5991 (1999).
[24] D. Primetzhofer, S. N. Markin, P. Zeppenfeld, P. Bauer, S. Prusa, M. Kolibal, and T. Sikola, Appl. Phys. Lett. **92**, 011929 (2008).
[25] J. Li, Z. Y. Wang, A. Tan, P.-A. Glans, E. Arenholz, C. Hwang, J. Shi, and Z. Q. Qiu, Phys. Rev. B **86**, 054430 (2012).
[26] W. Luo, S. J. Pennycook, and S. T. Pantelides, Phys. Rev. Lett. **101**, 247204 (2008).
[27] A. Verna, B. A. Davidson, Y. Szeto, A. Yu. Petrov, A. Mirone, A. Giglia, M. Mahne, and S. Nannarone, J. Magn. Magn. Mater. **322**, 1212 (2010).
[28] J. F. Ankner, C. F. Majkrzak, and H. Homma, J. Appl. Phys. **73**, 6436 (1993).
[29] R. L. Erickson and D. P. Smith, Phys. Rev. Lett. **34**, 297 (1975).
[30] N. H. Tolk, J. C. Tully, J. Kraus, C. W. White, and S. H. Neff, Phys. Rev. Lett. **36**, 747 (1976).
[31] A. Zartner, E. Taglauer, and W. Heiland, Phys. Rev. Lett. **40**, 1259 (1978).
[32] R. Souda, T. Aizawa, C. Oshima, S. Otani, and Y. Ishizawa, Phys. Rev. B **40**, 4119 (1989).
[33] D. Primetzhofer, M. Spitz, S. N. Markin, E. Taglauer, and P. Bauer, Phys. Rev. B **80**, 125425 (2009).
[34] T. T. Suzuki, H. Kuwahara, and Y. Yamauchi, Surf. Sci. **604**, 1767 (2010).
[35] M. Getzlaff, J. Bansmann, and G. Schonhense, J. Magn. Magn. Mater. **192**, 458 (1999).
[36] E. Yu, Tsymbal, I. I. Oleinik, and D. G. Pettifor, J. Appl. Phys. **87**, 5230 (2000).
[37] A. Tange, C. L. Gao, B. Yu. Yavorsky, I. V. Maznichenko, C. Etz, A. Ernst, W. Hergert, I. Mertig, W. Wulfhekel, and J. Kirschner, Phys. Rev. B **81**, 195410 (2010).